CONF-790745--1

TWO-PHASE FLOW MEASUREMENTS WITH ADVANCED INSTRUMENTED SPOOL PIECES AND LOCAL CONDUCTIVITY PROBES*

K. G. Turnage
C. E. Davis

Union Carbide Corporation Nuclear Division
Oak Ridge National Laboratory
Oak Ridge, TN 37830

ABSTRACT

A series of two-phase, air-water and steam-water tests performed with instrumented spool pieces and with conductivity probes obtained from Atomic Energy of Canada, Ltd. is described. The behavior of the three-beam densitometer, turbine meter, and drag flowmeter is discussed in terms of two-phase models. Application of some two-phase mass flow models to the recorded spool piece data is made and preliminary results are shown.

Velocity and void fraction information derived from the conductivity probes is presented and compared to velocities and void fractions obtained using the spool piece instrumentation.

Presented at Reactor Safety Instrumentation Review Group Meeting
Silver Spring, MD, July 25, 1979

---

*Research sponsored by Division of Reactor Safety Research, U. S. Nuclear Regulatory Commission under Interagency Agreements DOE 40-551-75 and 40-552-75 with the U.S. Department of Energy under contract W-7405-eng-26 with the Union Carbide Corporation.

1. INTRODUCTION

The measurement of two-phase mass flow rate is of primary importance in experimental programs involving loss-of-coolant studies. Because of the severe environments present during blowdown, relatively few instrument types have gained widespread acceptance; these include turbine meters, gamma densitometers, and drag flowmeters. (Pressure and temperature measurements are also required for reduction of data from the other instruments.)

In the Thermal-Hydraulic Test Facility (THTF) at Oak Ridge National Laboratory (ORNL)[1] and in the Semiscale facility at Idaho National Engineering Laboratory (INEL)[2], three full-flow instruments have been located in a relatively short piping segment called a spool piece. The design of spool pieces is important because the turbine meter and drag flowmeter are intrusive and may seriously alter the flow regime.[3] On the other hand, location of all three instruments in close proximity is desirable because of the often unsteady and inhomogeneous nature of two-phase flow.

During the previous year experimental work involved air-water testing of a spool piece which incorporated a three-beam gamma densitometer, a turbine flowmeter and two drag flowmeters with full-flow targets. A similar spool piece was tested in vertical upflow in the AIRS Test Stand, a steady-state steam-water flow system, which produces environments typical of the reflood portion of a postulated loss-of-coolant accident.

As part of the effort to understand the behavior of spool piece and impedance-type reflood instrumentation, studies were performed in the air-water loop with conductivity probes obtained from Canadian General Electric and Atomic Energy of Canada Limited (AECL).

This paper presents preliminary results from the air-water and steam-water spool piece experiments and from the signal analysis experiments.

2. AIR-WATER SPOOL PIECE STUDIES

The spool piece shown in Fig. 1 was installed in the ORNL Air-water test facility, and tested with two-phase horizontal flow[4,5], downflow[6] and upflow.[7] The purpose of the tests was to evaluate, for a wide range of air and water flow rates, the performance of the spool piece in terms of readily available analytical techniques. Of particular interest was the use of larger drag target designs, which sample the flow to within 3.2 mm of the pipe wall. The effects of such targets on the flow pattern detected by the three-beam densitometer were studied and comparisons of velocities predicted by the Aya, Rouhani, and volumetric models of turbine behavior to reduced turbine readings were made. Information gained from studies of each spool piece instrument was used to evaluate the results of two-phase mass flow models that require the instrument readings.

2.1 Experiment Description

The instrumented spool piece used in the air-water studies (Fig. 1) incorporates several design improvements: (1) The upstream drag flowmeter (normal flow direction), the densitometer, and the turbine are located within 46 cm (18 in) of each other. (2) Location of a drag flowmeter on either end allows one drag meter to always be upstream of the turbine in case of bidirectional flow. (3) The "full-flow" turbine rotor and drag flowmeter targets used sample the fluid flow in the pipe to within 3.2 mm (0.125 in) of the pipe wall. And (4) Fast response, high sensitivity turbine monitor electronics developed at ORNL were used with the turbine meter.

Detailed descriptions of the spool piece instrumentation, signal conditioning equipment and data acquisition methods used are reported elsewhere[4,5].

The ORNL two-phase air-water loop (Fig. 2) is capable of supplying air at flow rates up to 242 liters/sec (512 scfm) and water at flow rates up to 32 liters/sec (500 gpm). In the 8.9-cm-ID (3.5-in.) spool piece tested, those rates correspond to superficial velocities of 39 m/sec (128 fps) for air and 5.2 m/sec (17 fps) for water. The air and water flow was at ambient temperature and near atmospheric pressure. In the air-water loop, air flow rate is determined using a pressure gage upstream of critical flow orifices, and water is metered into the loop by means of rotameters flow rates [6.3 liters/sec (100 gpm)] or by a magnetic flowmeter.

The spool piece was tested in the facility in the three locations shown in Fig. 2. By adjustment of valves, two-phase flow was made to pass horizontally, vertically upward or vertically downward through the test section.

Experiments were conducted by setting the desired air flow rate and then taking data at successively higher water input rates until either the system pressure became high enough to unchoke the critical flow orifice or one of the instruments was overranged. The air flow rate was then doubled, and the procedure of taking data with various water flow rates was repeated.

The flow rates used resulted in many two-phase flow regimes (Figs. 3, 4, and 5). The flow regimes observed through the transparent loop piping at various flow rates generally agreed with those indicated by Mandhane and Aziz[8] (Fig. 3) and by Oshinowa and Charles[9] (Figs. 4 and 5).

The spool piece instrumentation was calibrated in single-phase flow immediately prior to each two-phase test. Simple equations[5] were then used to reduce the turbine and drag flowmeter data recorded from the two-phase tests, yielding a velocity V_t from the turbine and a momentum flux I_d indicated by the drag flowmeter. A mean pipe density ρ_a was deduced from the three-beam densitometer data using models which postulated three regions, each with uniform density. An "annular" model (Fig. 6) was used with the vertical upflow and vertical downflow data and a "stratified" model (Fig. 7) was used to reduce data from the horizontal tests. Lucite inserts representing various flow regimes (Fig. 8) were used to verify the accuracy of the density measurements.

The FORTRAN computer program used to process the raw data tapes calculated V_t, I_d, ρ_a and the pressure for short intervals of real time (≈0.1 sec). These "instantaneous" quantities were used to evaluate modeling expressions at a great many times for each flow rate. The short-time interval modeling expressions were then averaged over time to yield the numbers presented here. This method is appropriate for evaluation of models and instrumentation intended for transient or slug flow application.

2.2 Individual Instrument Response

A summary of results obtained with the triple-beam densitometer, turbine flowmeter and drag flowmeter in the air-water, two-phase flowtests is presented here. Where the spool piece orientation, e.g., horizontal vs. downflow had a significant effect on instrument behavior, the differences are indicated.

A transparent plexiglass spool piece of identical dimensions to the steel test section was used for visual studies of how the drag bodies and the turbine meter perturbed the flow. The studies revealed that when full-flow drag targets were used in advanced spool piece I, considerable disturbance of the flow regime occurred at the plane of the densitometer. The calculated composite densities were most seriously affected at the lowest void fractions when use of large targets apparently caused underestimates of the density by annular and stratified models. In vertical downflow (Fig. 9) when a full-flow drag target was mounted on the upstream drag flowmeter, a pronounced discontinuity in calculated density occurred at the transition from bubbly slug to coring bubble flow. If full-flow drag targets are to be used, they should be positioned downstream of the densitometer because the discontinuity did not occur without the drag target.

Analysis of data from the upflow experiments showed that there was no apparent effect on the composite density calculated using the densitometer, when a full-flow drag target was located upstream of the densitometer.

A study was made in which mean phase velocities (based on metered inputs and densitometer data) were substituted into expressions for theturbine velocity postulated by Aya[10], Rouhani[11], and the volumetric[12] model. Comparisons between the turbine speeds predicted by the models and mean turbine speeds recorded in horizontal flow (Fig. 10) revealed that the Aya and the Rouhani models perform well, with the Rouhani model doing slightly better.

In vertical downflow the slip ratios may be significantly less than unity because of gravitational and buoyancy effects. When $S < 1$, the turbine meter velocity may be less than both the mean liquid and the mean vapor velocities. The Aya and Rouhani turbine models (Fig. 11) simulate actual turbine behavior poorly at those flow rates, but they perform satisfactorily at high air flow rates when $S \gtrsim 1$. The volumetric turbine model was the most successful of the three models when $S < 1$. When data recorded in vertical upflow was used, (Fig. 13), the volumetric turbine model was found to greatly overpredict the turbine velocity at all flow rates. The Aya and the Rouhani turbine models predicted the turbine speed reasonably well over most of the range of flow rates used, except that they tended to underpredict the speed at high air flow rates with low water flow rates (high void fraction).

The momentum flux indicated by the drag flowmeter I_d was calculated using single-phase calibration factors and drag transducer output. This was compared to a two-velocity momentum flux based on either turbine meter or density data

and metered inputs to the loop.

In horizontal flow (Fig. 13) and in vertical downflow at flow rates where the calculated standards were deemed reliable, the two-phase drag coefficient appeared to be less than the single-phase C_D by ≈20%. This suggests that the accumulation of a vapor pocket just downstream of the drag target (Fig. 14), observed in high-speed motion pictures made through the transparent spool piece, causes a significant reduction in drag. Hoerner[13] has presented data showing the reduction in drag which occurs due to accumulation of a vapor pocket behind a bluff body.

For the vertical upflow tests, the two-phase drag coefficient of the four-bladed drag target appeared to approximate the single-phase value.

2.3 Two-Phase Mass Flow Rate Models

Calculations of the two-phase mass flux made with data from spool piece instrumentation were compared to the actual fluxes based on metered-in flow rates.

Comparisons of data calculated using the mass flow models $G_1 = \rho_a V_t$, $G_2 = \sqrt{\rho_a I_d}$, and $G_3 = I_d/V_t$ to the actual two-phase mass flux have suggested the following:

1. G_1 (Fig. 15) is reliable when the turbine velocity approximates the liquid velocity (Fig. 16), particularly when the void fraction is less than 50%. G_1 increasingly overpredicts the true mass flux at higher void fraction.

2. G_2 (Fig. 17) is reliable when the water superficial velocity is high, but it tends to overpredict the correct mass flux at low liquid flow rates.

3. G_3 (Fig. 18) was found to yield consistent mass flux calculations with respect to the actual values. (G_3 conforms to a two-velocity assumption, if the Rouhani-Estrada turbine model is used.) In horizontal flow and in downflow, G_3 usually underestimated the correct mass flux by some 10-30 per cent, perhaps because of variations in the two-phase flow drag coefficients from the single-phase values.

3. STEAM-WATER SPOOL PIECE TESTS

The AIRS Test Stand tests were conducted to examine how observations made in the air-water experiment regarding instrument response and mass flow rate determination translate to a steam-water flow system. In particular, we wanted to determine whether the mass flow rate in two-phase steam water flow could be obtained with sufficient accuracy using only a drag flowmeter and a turbine flowmeter. (If so, useful instrumented spool pieces could be constructed without using relatively expensive gamma attenuation densitometers.)

This section briefly describes the AIRS Test Stand and the methods of data acquisition and analysis used for the spool piece tests. Results from preliminary analysis of the data are discussed.

3.1 Experimental Equipment and Methods

The Advanced Instruments for Reflood Studies (AIRS) Steam-Water Test Stand (Fig. 19) is used for testing instrument systems in flow conditions like those in a postulated nuclear reactor reflood. Superheated steam at 830 kPa (120 psia) and 440 K (340°F) water at ambient temperature and pressure are mixed and passed vertically upward through piping where flow instruments are located. Input flow rates of each phase to the system are measured using rotometers for water input and a Gilflo steam flowmeter for steam input. Visual observations of the mixed flow stream may be made both upstream and downstream of the test sections. An instrumented piping spool piece is located near the top of the facility; measurements made with the spool piece instrumentation are compared to analogous measurements obtained with impedance probes or other devices installed in the lower sections.

The instrumented spool piece used for the steam-water testing (Fig. 20) consisted of a 91-cm. long (3.0 ft.), 8.9 cm. ID (3.5 in.) stainless steel pipe with fittings for a drag flowmeter and a turbine meter. A triple-beam gamma attenuation densitometer was installed on the spool piece at the location shown in Fig. 20.

The two-phase flow tests described here are summarized in Table 3.1. The tests were performed at a spool piece pressure of ≈725kPa (≈105 psia). An energy balance was applied to the input flow rates and enthalpies to obtain the mixture quality at the spool piece. For the flow rates used, the calculated test section quality was between 0.0004 and 0.48, while the void fraction in the spool piece, derived using the densitometer data, ranged from 0.66 to 0.99.

Table 3.1. Two-Phase Flow Conditions for AIRS Test Stand Steam-Water Tests

Superficial Liquid velocity m/sec	(ft/sec)	Superficial Vapor velocity m/sec	(ft/sec)	Quality %	Void Fraction[a] %
0.25	(0.81)	0.23	(0.74)	0.4	59
0.25	(0.83)	2.1	(7.07)	3.4	73
0.25	(0.82)	5.0	(16.00)	7.7	81
0.25	(0.82)	10.0	(33.00)	15.0	93
0.25	(0.81)	19.0	(63.00)	24.0	95
0.17	(0.57)	0.39	(1.30)	0.9	63
0.17	(0.57)	2.3	(7.60)	5.3	76
0.17	(0.57)	5.5	(18.00)	12.0	84
0.17	(0.57)	13.0	(42.00)	24.0	95
0.12	(0.38)	15.0	(50.00)	36.0	96
0.11	(0.36)	6.5	(21.00)	19.0	90
0.12	(0.38)	2.4	(8.00)	8.1	75
0.12	(0.38)	0.88	(2.90)	3.1	60
0.073	(0.24)	1.7	(5.60)	9.0	70
0.073	(0.24)	3.7	(12.00)	18.0	83
0.073	(0.24)	6.2	(20.00)	26.0	89
0.073	(0.24)	16.0	(52.00)	48.0	96

[a]Based on gamma densitometer data.

The flow rates were chosen to allow examination of unsteady, slug flow regimes (low steam flow rates) as well as annular mist flow regimes (high steam flow rates).

3.2 Steam-Water Test Results

Analysis of the densitometer data showed that the pipe-average slip ratios for the steam-water flow points were high, ranging from ≈3 to ≈10. The turbine velocity was found to greatly exceed the mean liquid phase velocity; its velocity was fairly close to the mean steam velocity over most of the flow range. Consequently, the Aya and the Rouhani turbine models seriously underestimated the turbine velocities for these tests. The volumetric model, however, predicted the turbine velocity reasonably well, except at the lowest steam flow rates used. (The 12-bladed turbine used in the steam-water tests was also found to greatly overestimate the liquid velocity in the air-water system, in contrast to the 5-bladed turbine used previously.)

Comparisons of the data calculated using the mass flow models $G_1 = \rho_a V_t$, $G_2 = \sqrt{\rho_a I_d}$, and $G_3 = I_d/V_t$, to the actual two-phase mass flux in vertical upflow, have suggested the following:

1. At the flow rates and void fractions used in the steam-flow tests, G_1 grossly overestimates the mass flux (Fig. 21), largely due to turbine speeds well in excess of the mean liquid velocity.

2. G_2 overestimates the mass flux at the high slip ratios characteristic of the steam water tests (Fig. 22), though not as badly as does G_1.

3. When the drag flowmeter output was high enough to be significant, G_3 was found to yield consistent results, but falling somewhat below the true mass flux because of the turbine overspeed problem mentioned above (Fig 23).

4. AECL CONDUCTIVITY PROBES

Three conductivity probes which were designed and fabricated by Canadian General Electric and Atomic Energy of Canada Limited (AECL) were installed in a 0.46-m-long transparent spool piece and tested in vertical upflow in the air-water test facility.[7] The AECL conductivity probe tests were to examine the performance of the probes in various air-water flow rates and different flow regimes, and to compare their measurements with other commonly used instruments in two-phase flow. The probes' operation is based on the fact that the conductivity of air is less than that of water, thus the probes are able to detect the passage of an air bubble or a water droplet. Two different types of conductivity probes have been designed and build by AECL[14]: one to measure velocity (Fig. 24 top) and the other to measure void fraction (Fig. 24 bottom) in two-phase flow.

Two different velocity probes have been tested, one with a prong separation distance of 4 mm and the other a separation of 3 mm. A preliminary spectral analysis of the signals from both the 3-mm and the 4-mm velocity probes showed that good coherence of the signals and repeatable velocities could be obtained. A thorough test of the velocity probes using sixteen different air-water flow rate combinations ranging from 0.6 to 25.2 ℓ/s (10 to 400 gpm) of water and from 1.9 to 241.7 ℓ/s (45 to 512 scfm) of air and several different flow regimes (Table 4.1) was conducted.

The velocity probes gave unambiguous readings at all flow rates tested, at void fractions ranging from 3 to 98%. The velocities generally agreed with the turbine meter speed (Fig. 25) in the bubble, slug and froth flow regimes, but the probes indicated somewhat lower velocities than the turbine in annular flow. The manner in which the probe cross correlation velocities compared to the mean phase velocities V_f and V_g (based on densitometer data and metered flow rates) may be seen in Table 4.1.

The AECL void fraction probe, which consists of five separate sensing points along the diameter of the pipe, was tested under the same flow rates and flow regimes as was the 4-mm velocity probe. The void fraction probe was compared to the void fractions determined with a three-beam gamma densitometer. The void fraction for each of the 5 points on the probe in calculated using Eq. (4.1)

$$\alpha_i = \frac{RMS_\ell - RMS_{2\phi}}{RMS_\ell - RMS_G} \qquad (4.1)$$

Table 4.1. Experimental data from air-water tests with AECL velocity probes and advanced spool piece 1

Water flow rate (gpm)	Air flow rate (scfm)	Vel probe (ft/sec)	Vel T.M. (ft/sec)	% diff $(1 - \frac{Vp}{VTM})$ X100	Flow regime[a]	V_g ft/sec	V_f ft/sec	Void fraction γ-densitometer
40	4	3.20	4.62	30.8	Quiet slug	3.67	1.96	0.27
100	4	5.68	4.56	-24.6	Quiet slug	5.38	4.34	0.19
200	4	8.53	8.01	-6.5	Bubble	7.85	7.79	0.13
300	4	10.93	11.34	3.6	Bubble	11.40	11.00	0.09
400	2	13.99	13.71	-2.0	Bubble	15.28	13.80	0.03
20	16	5.22	6.09	14.2	Dispersed slug	7.26	1.63	0.55
40	16	5.19	4.70	-10.4	Dispersed slug	7.97	3.01	0.50
100	16	6.90	5.60	-23.1	Dispersed slug	11.59	5.66	0.34
20	64	9.96	5.42	-83.7	Frothy slug	21.98	2.54	0.73
60	64	11.36	7.64	-48.7	Frothy slug	24.01	6.20	0.66
300	64	15.09	17.73	14.9	Frothy slug	38.92	17.20	0.41
100	128	13.12	14.80	11.3	Frothy slug	43.13	13.24	0.74
60	256	19.69	19.68	0.0	Froth	75.71	13.21	0.84
60	512	24.13	38.24	36.9	Annular	140.6	22.73	0.91
40	512	30.10	42.20	28.7	Annular	136.9	20.78	0.93
10	512	40.69	69.33	41.3	Annular	130.4	16.28	0.98

[a] Based on flow regime map of Oshinawa and Charles.[3]

The root mean square (RMS) value of the signal from the probe was determined with a Hewlett-Packard model 54-20 spectrum analyzer. The individual void fractions from each probe tip are averaged to give each signal its proper weight according to its position along the pipe centerline. The average void fraction for the pipe cross section is thus calculated by Eq. (4.2)

$$\bar{\alpha} = 1/3 \left[\left(\frac{\alpha_A + \alpha_E}{2} \right) + \left(\frac{\alpha_B + \alpha_D}{2} \right) + \alpha_C \right] , \qquad (4.2)$$

where the subscripts refer to tip positions shown in Fig. 4.2.

Using air-water data, the five-point void fraction probe gave pipe-average void fractions which always agreed with the three-beam densitometer within 20% of reading (Fig. 26). Radial void profiles obtained with the probe were characteristic of a particular flow regime and generally had a symmetric shape about the pipe axis (Fig. 27).

SUMMARY

Experiments performed in air-water and steam-water two-phase flow with improved instrumented spool pieces have yielded significant results regarding interpretation of densitometer and turbine and drag flowmeter data. Models commonly used to calculate mass flow may be adequate at low void fraction when slip ratios are near unity, but the models are inaccurate under other conditions. At high void fractions, the model $G_3 = I_d/V_t$ is the most reliable. Results from vertical upflow, high void fraction steam-water experiments generally agreed with the air-water results.

Velocity and void fraction measurements were made in the air-water system with local conductivity probes, in conjunction with vertical upflow spool piece tests. The velocity probe cross-corrolation velocities approximated the mean turbine velocities except in annular flow. Measurements made with the void fraction probe agreed well with the densitometer measurements and provided information regarding void profiles in the pipe.

REFERENCES

1. "Project Description ORNL-PWR Blowdown Heat Transfer Separate-Effects Program - Thermal-Hydraulic Test Facility." ORNL/NUREG.TM-218 (NUREG/CR-0104) (1978).

2. E. M. Feldman and D. J. Olson, *Semiscale MOD-1 Program and System Description for the Blowdown Heat Transfer Tests (Test Series 2)*, Idaho National Engineering Laboratory Report No. ANCR-1230 (August 1975).

3. J. D. Sheppard, P. H. Hayes, and M. C. Wynn, "An Experimental Study of Flow Monitoring Instruments in Air-Water Two-Phase Downflow," presented at OECD/NEA Symposium on Transient Two-Phase Flow, Toronto, Canada, August 1976.

4. K. G. Turnage, et al., *Advanced Two-Phase Instrumentation Program Quarterly Progress Report for April-June 1978*, ORNL/NUREG/TM-279 (January 1979).

5. K. G. Turnage, et al., *Advanced Two-Phase Flow Instrumentation Program Quarterly Progress Report for July-September 1978*, ORNL/NUREG/TM-309 (May 1979).

6. K. G. Turnage, et al., *Advanced Two-Phase Flow Instrumentation Program Quarterly Progress Report for October-December 1978*, ORNL/NUREG/TM-313 (May 1979).

7. K. G. Turnage, et al., *Advanced Two-Phase Flow Instrumentation Program Quarterly Progress Report for January-March 1979*, ORNL/NUREG/TM-331 (In Press).

8. J. D. Mandhane, et al., "A Flow Pattern Map for Gas-Liquid Flow in Horizontal Pipes," *Int. J. Multiphase Flow* 1, 537-53 (1974).

9. T. Oshinowo and M. E. Charles, "Vertical Two-Phase Flow, Part I. Flow Pattern Correlations," *Can. J. Chem. Eng.* 53,25 (1974).

10. Izuo Aya, *A Model to Calculate Mass Flow Rate and Other Quantities of Two-Phase Flow in a Pipe with a Densitometer, a Drag Disk, and a Turbine Meter*, ORNL/TM-4759 (November 1975).

11. S. Z. Rouhani, "Application of the Turbine Type Flowmeters in the Measurements of Steam Quality and Void," *Symposium of In-Core Instrumentation, Oslo, Norway, June 1974.*

12. S. Silverman, *Principles of Operation and Data Reduction Techniques for the LOFT Drag Disc Turbine Transducer*, TREE-NUREG-1109, p. 33 (1977).

13. S. F. Hoerner, Fluid Dynamic Drag, 2nd Ed., p. 10-7, Hoerner Fluid Dynamics, Brick Town, N. J. 08723

14. R. S. Flemons, et al., "Conductivity Probes for Void and Velocity Measurements in High Temperature Steam-Water Flow," 25th International Instrumentation Symposium, Anaheim, CA, (May 1979).

UNION CARBIDE
ORNL

ADVANCED SPOOL PIECE 1

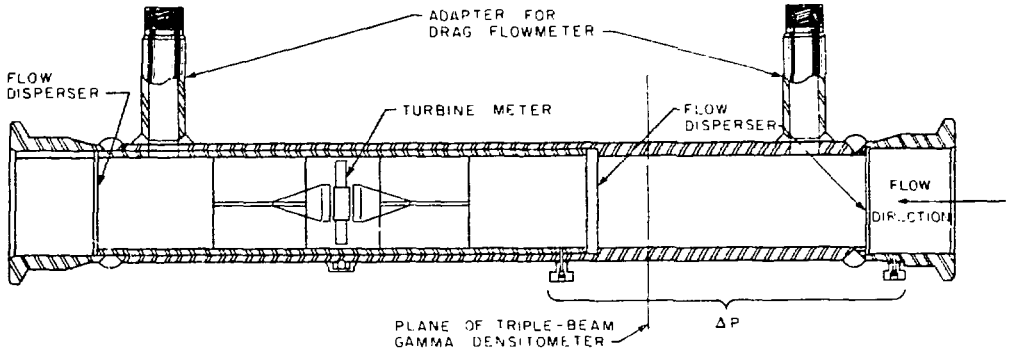

FIG. 1. INSTRUMENTED PIPING SPOOL PIECE USED IN AIR-WATER TESTING.

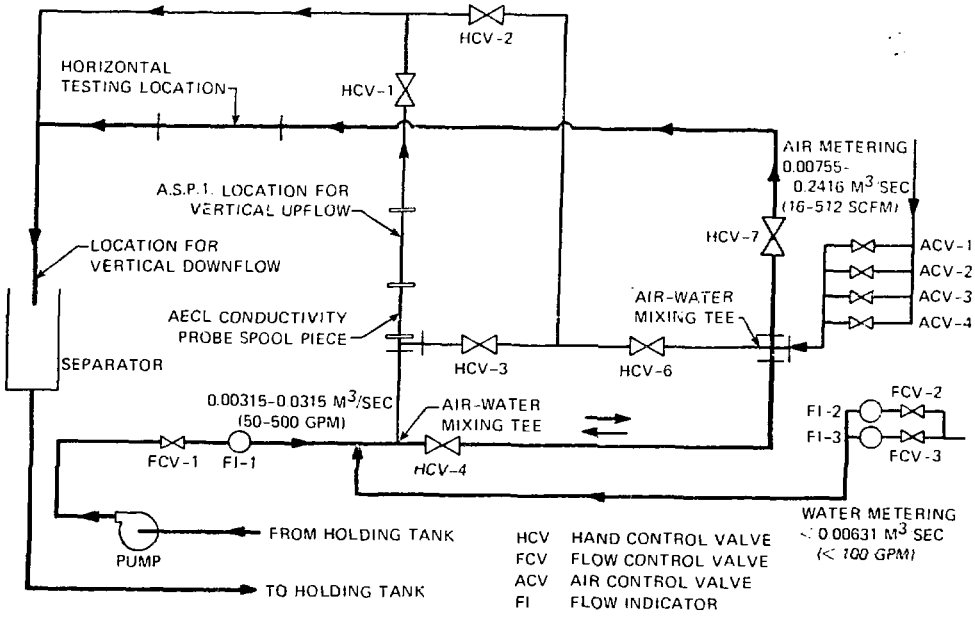

FIG. 2. ORNL AIR-WATER TEST FACILITY.

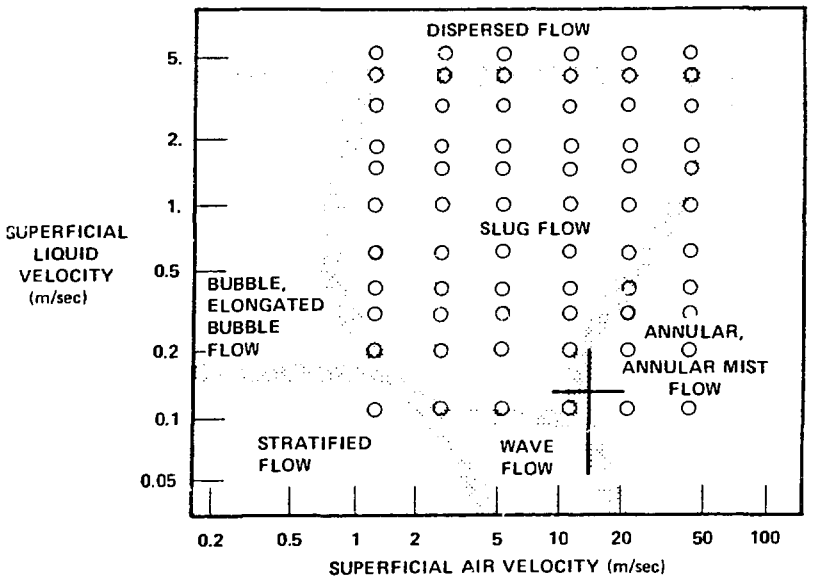

FLOW REGIME MAP OF MANDHANE AND AZIZ (1974)

FIG. 3. FLOW PATTERN MAP PROPOSED BY MANDHANE, ET AL., FOR HORIZONTAL FLOW WITH LOCATIONS OF DATA POINTS USED IN AIR-WATER STUDIES.

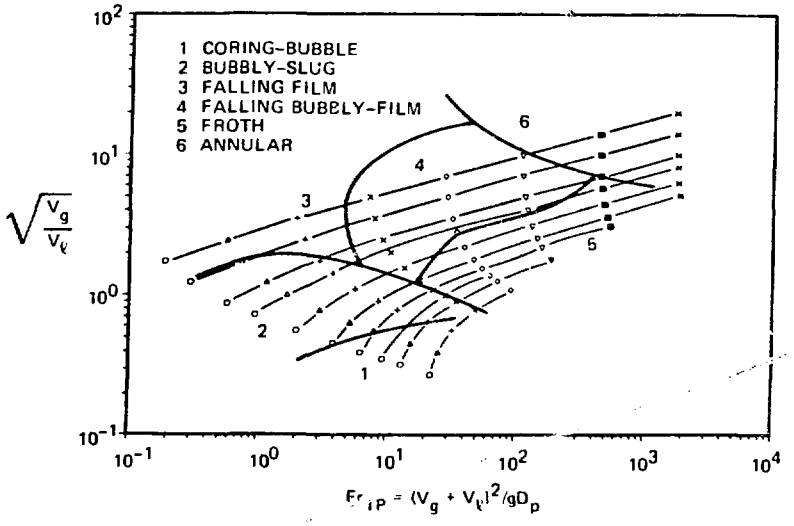

FLOW REGIME MAP OF OSHINOWO AND CHARLES (1974)

FIG. 4. FLOW PATTERN MAP PROPOSED BY OSHINOWA AND CHARLES FOR VERTICAL DOWNFLOW WITH LOCATIONS OF DATA POINTS USED IN AIR-WATER STUDIES.

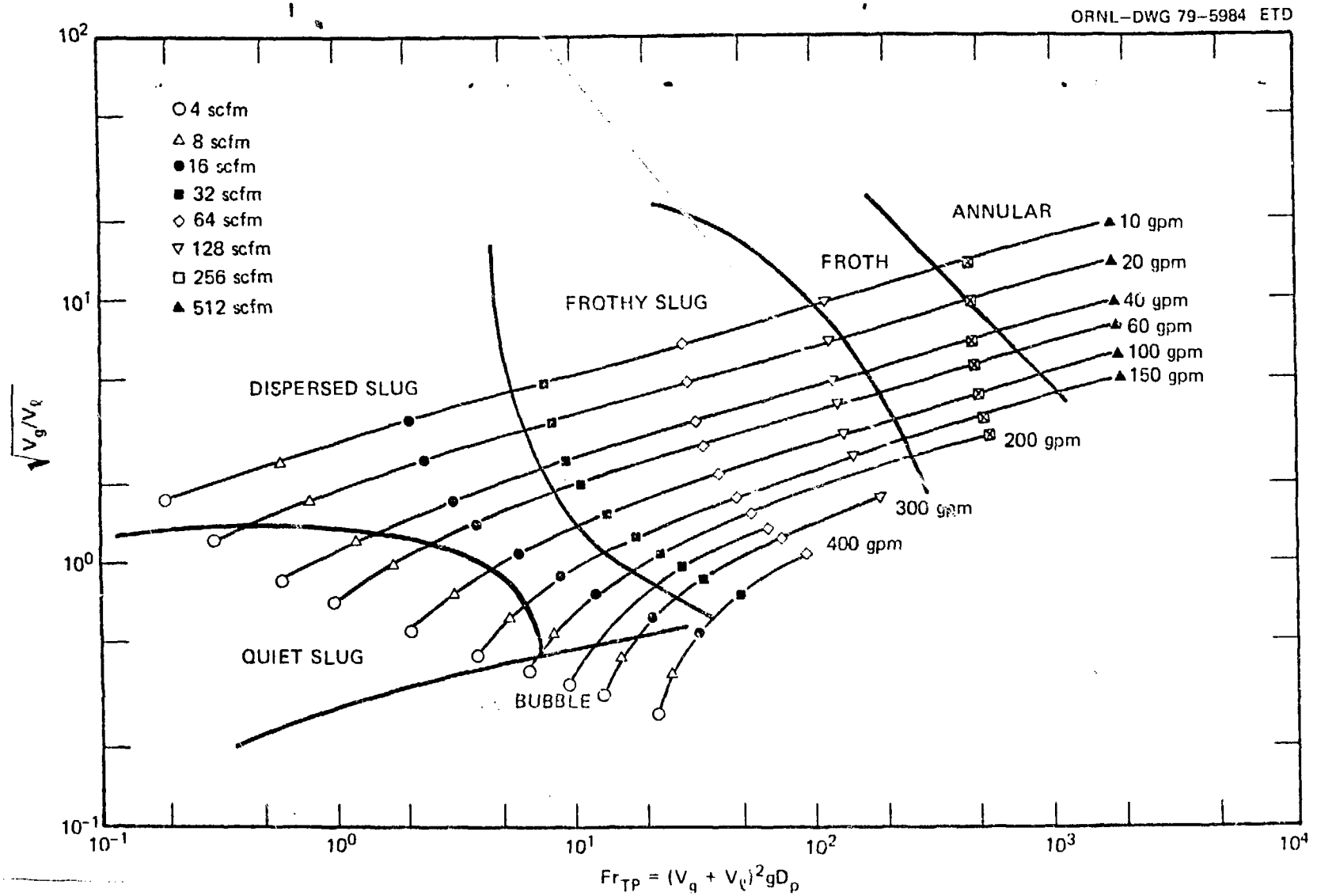

FIG. 5. FLOW PATTERN MAP PROPOSED BY OSHINOWA AND CHARLES FOR VERTICAL UPFLOW WITH LOCATIONS OF DATA POINTS USED IN AIR-WATER STUDIES.

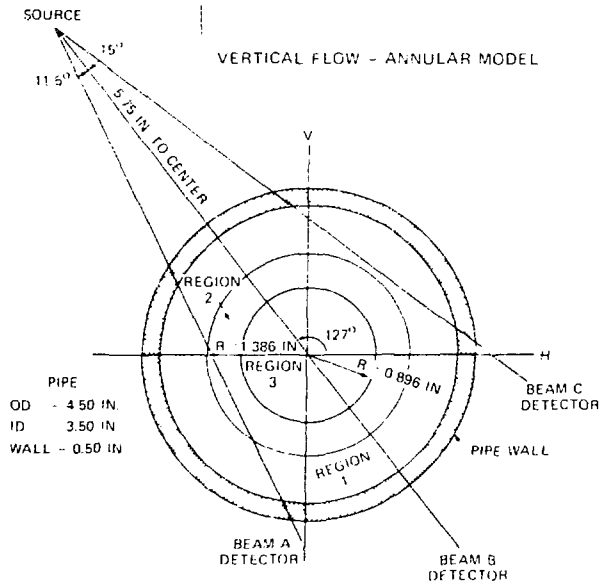

FIG. 6. DIAGRAM SHOWING UNIFORM DENSITY REGIONS USED IN ANNULAR MODEL FOR REDUCTION OF THREE-BEAM DENSITOMETER DATA.

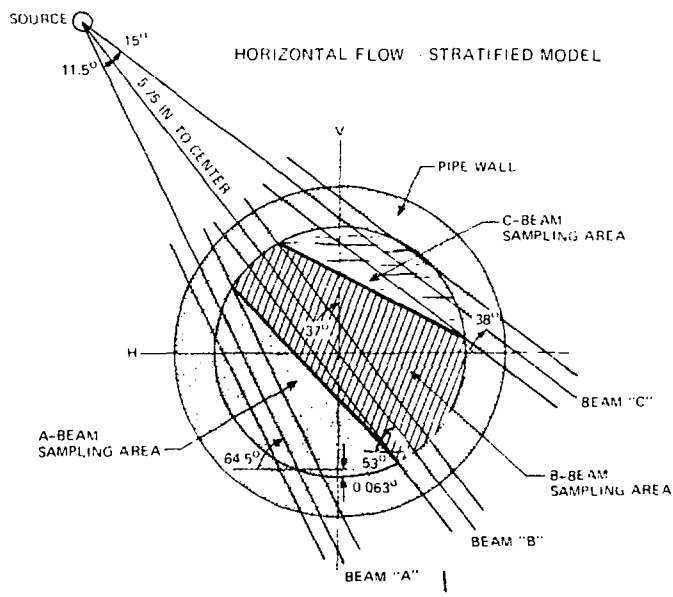

FIG. 7. DIAGRAM SHOWING UNIFORM DENSITY REGIONS USED IN STRATIFIED MODEL FOR REDUCTION OF THREE-BEAM DENSITOMETER DATA.

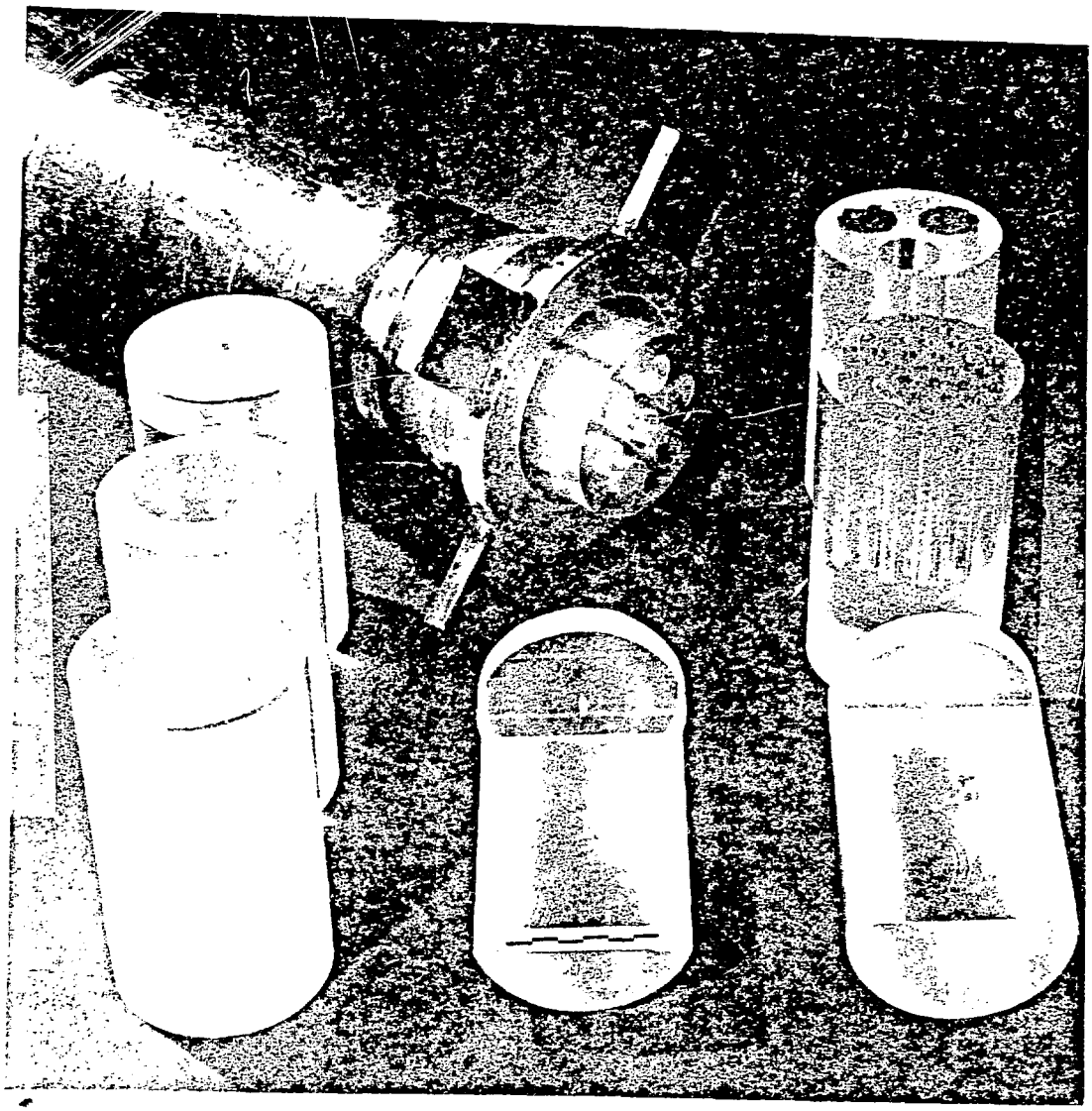

FIG. 8. PLEXIGLASS INSERTS REPRESENTING TWO-PHASE FLOW REGIMES. USED TO EVALUATE ACCURACY OF DENSITOMETER MEASUREMENTS.

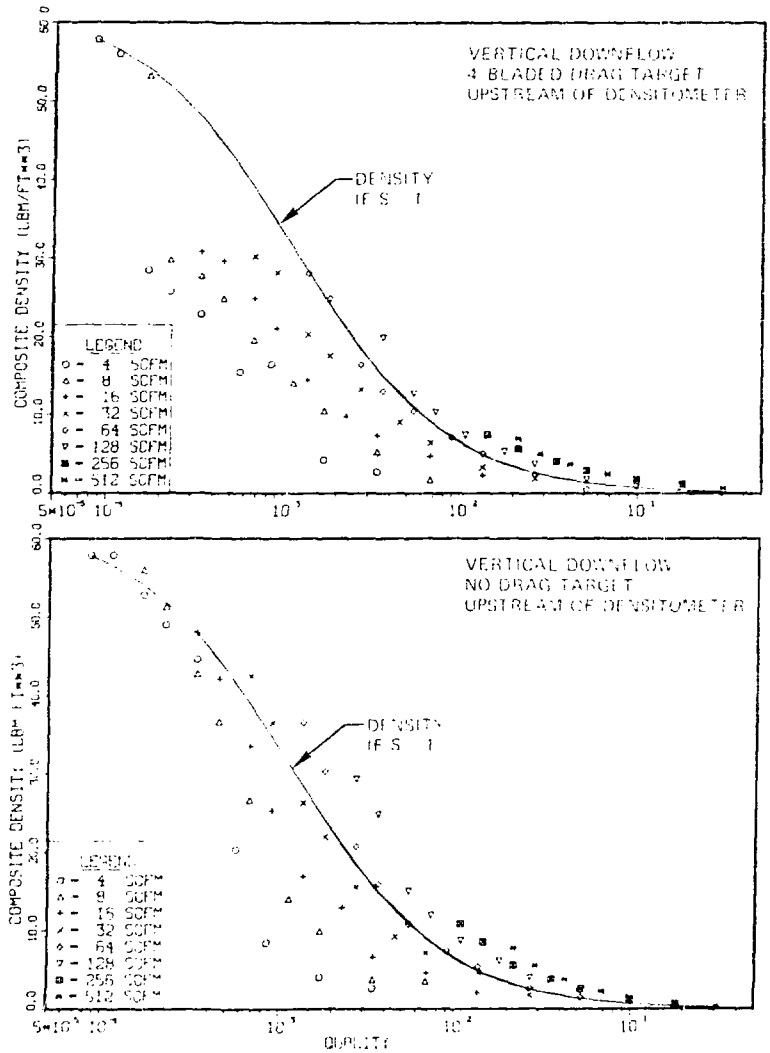

FIG. 9. COMPARISON SHOWING EFFECTS OF LOCATION OF FULL-FLOW DRAG TARGET UPSTREAM OF DENSITOMETER IN AIR-WATER VERTICAL DOWNFLOW.

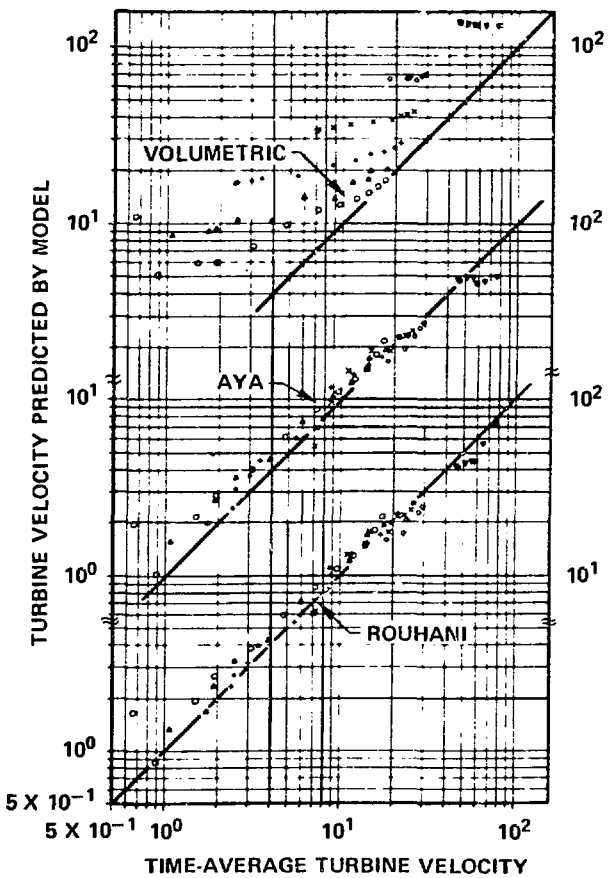

FIG. 10. TURBINE VELOCITY PREDICTED BY THREE TURBINE MODELS VS ACTUAL MEAN TURBINE VELOCITY RECORDED IN HORIZONTAL FLOW. SOLID LINES DENOTE PERFECT AGREEMENT FOR EACH MODEL.

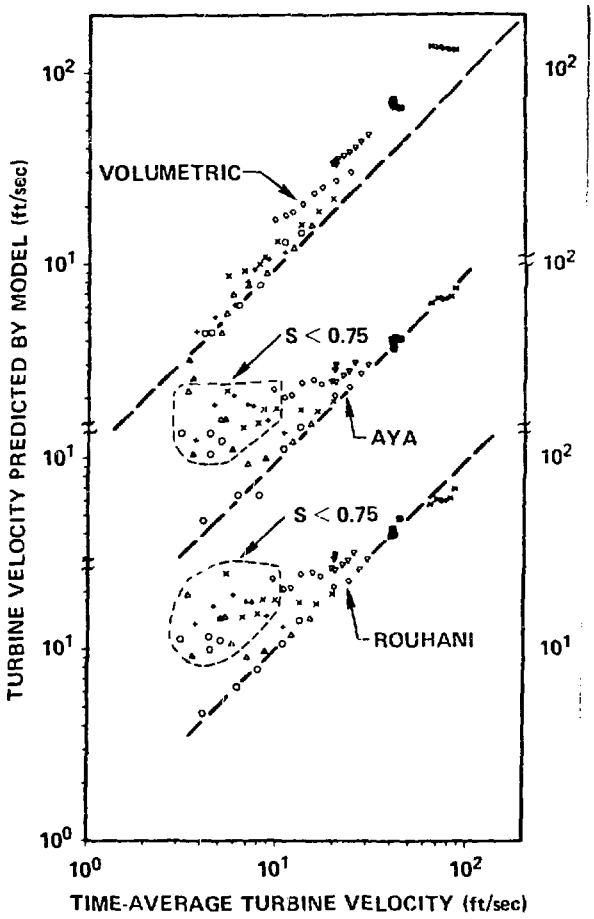

FIG. 11. TURBINE VELOCITY PREDICTED BY THREE TURBINE MODELS VS *ACTUAL MEAN TURBINE VELOCITY RECORDED IN VERTICAL DOWNFLOW.* SOLID LINES DENOTE PERFECT AGREEMENT FOR EACH MODEL.

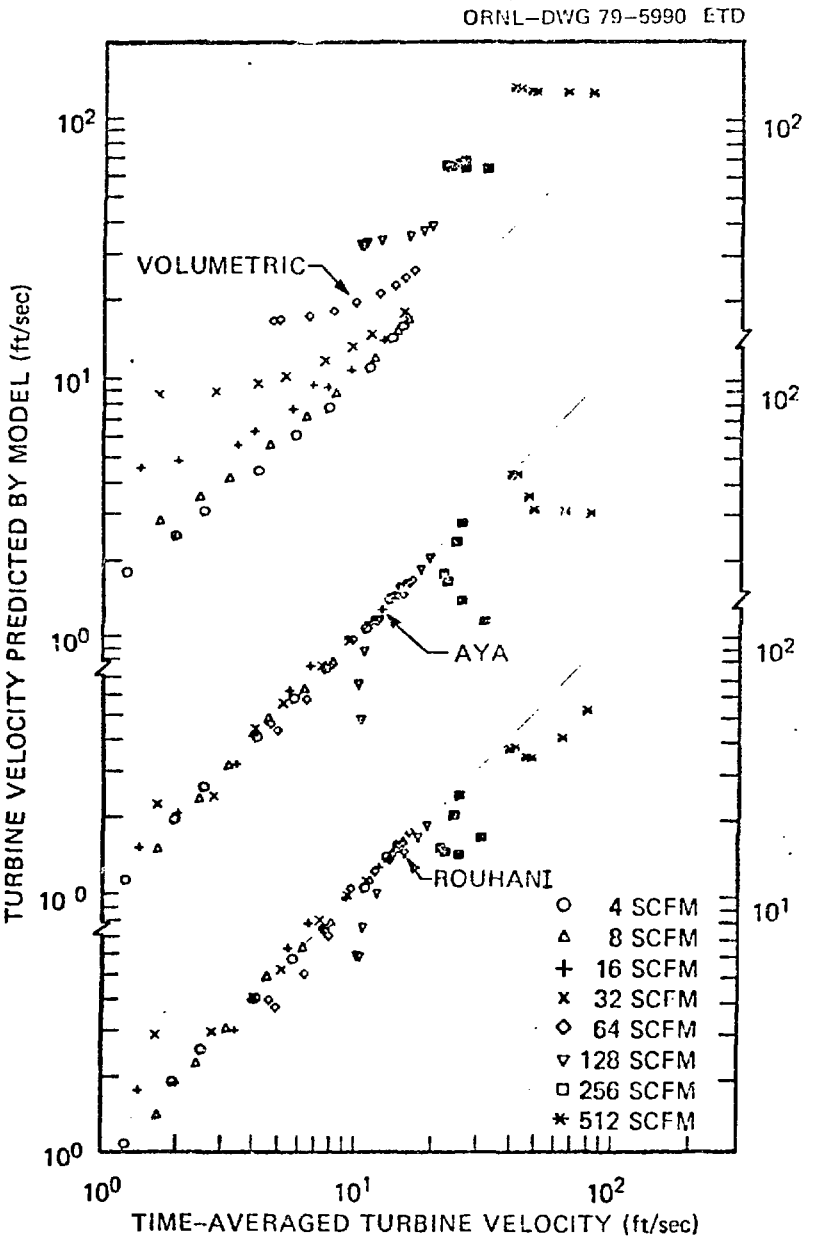

FIG. 12. TURBINE VELOCITY PREDICTED BY THREE TURBINE MODELS VS ACTUAL MEAN TURBINE VELOCITY RECORDED IN VERTICAL UPFLOW. SOLID LINES DENOTE PERFECT AGREEMENT FOR EACH MODEL.

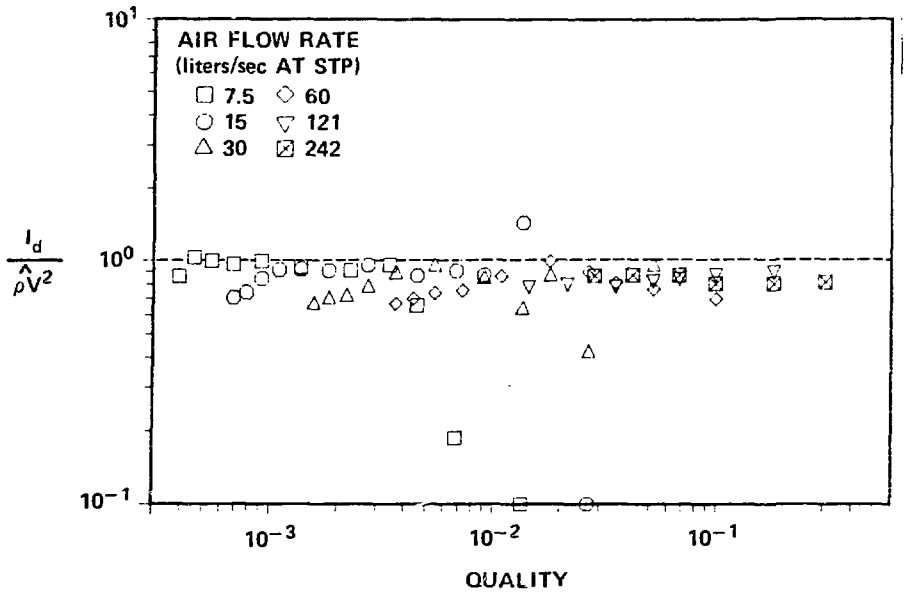

FIG. 13. RATIO OF MOMENTUM FLUX INDICATED BY DRAG FLOWMETER TO MOMENTUM FLUX CALCULATED USING METERED FLOW RATES AND TURBINE VELOCITY (HORIZONTAL FLOW, PERFORATED PLATE TARGET).

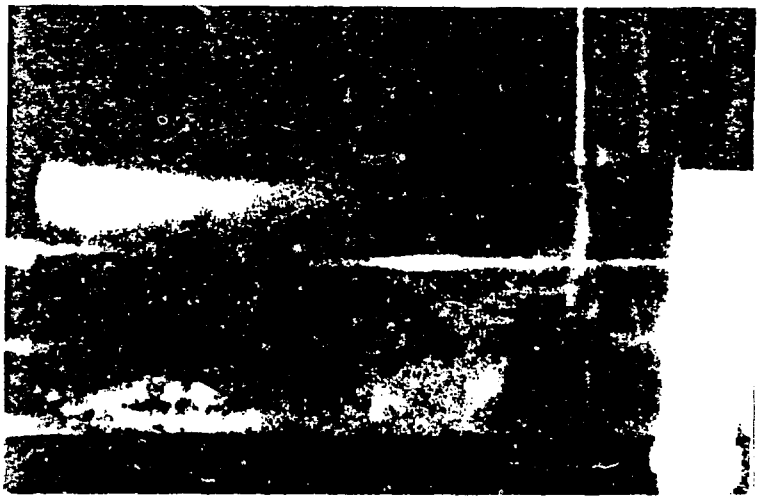

FIG. 14. PHOTOGRAPH MADE THROUGH TRANSPARENT SPOOL PIECE SHOWING WAKE REGION OCCURING DOWNSTREAM OF FOUR-BLADED DRAG TARGET. FLOW IS FROM RIGHT TO LEFT.

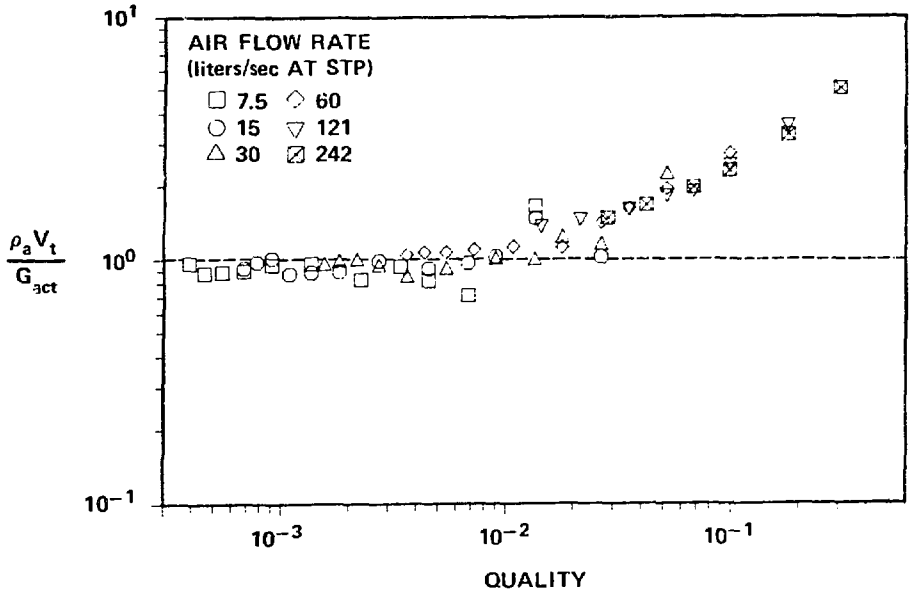

FIG. 15. RATIO OF MASS FLUX DETERMINED USING DENSITOMETER AND TURBINE TO ACTUAL MASS FLUX IN HORIZONTAL TWO-PHASE FLOW.

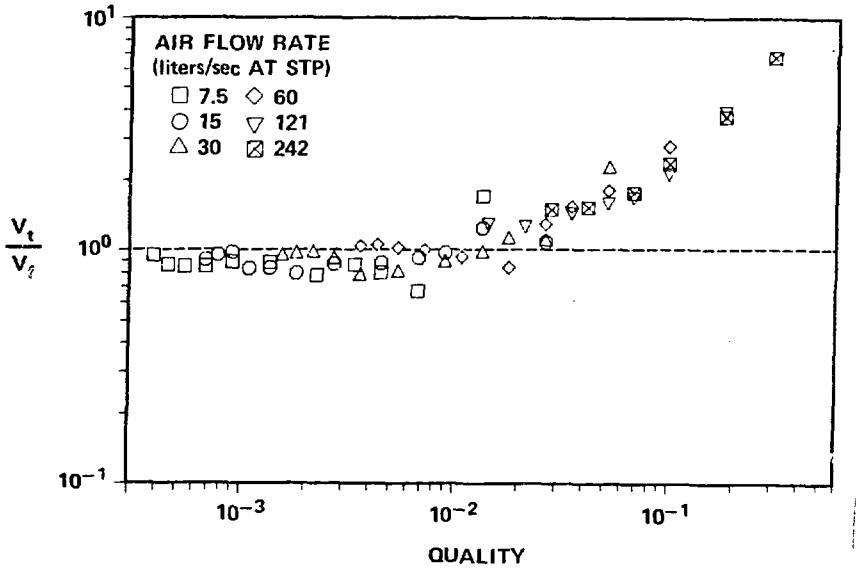

FIG. 16. RATIO OF TURBINE SPEED TO MEAN LIQUID PHASE VELOCITY IN HORIZONTAL TWO-PHASE FLOW.

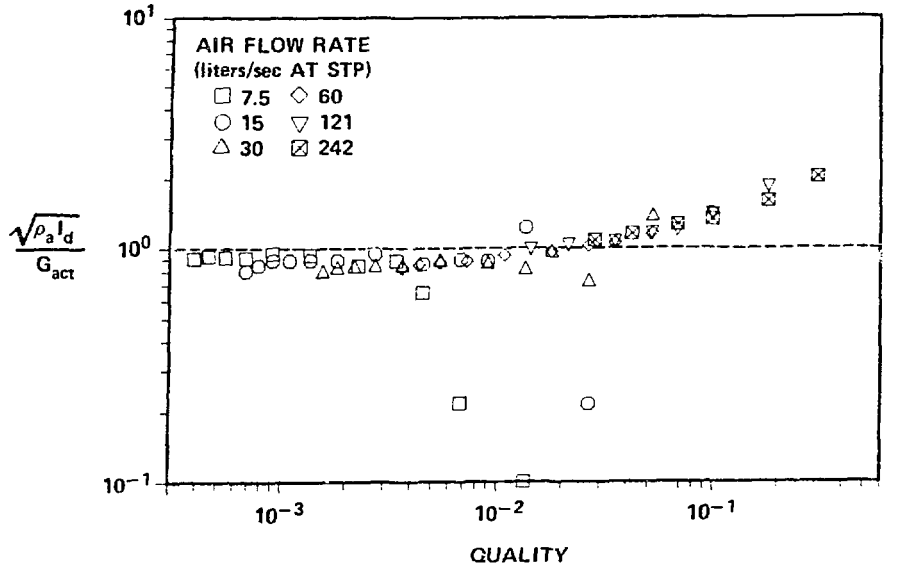

FIG. 17. RATIO OF MASS FLUX DETERMINED USING DENSITOMETER AND DRAG FLOWMETER TO ACTUAL MASS FLUX IN HORIZONTAL TWO-PHASE FLOW.

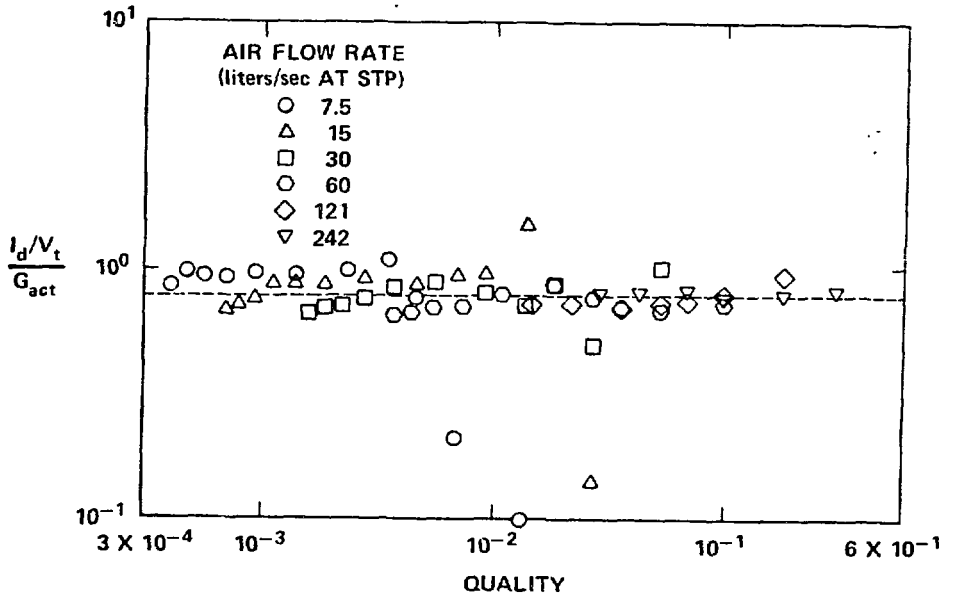

FIG. 18. RATIO OF MASS FLUX DETERMINED USING TURBINE AND DRAG FLOWMETER TO ACTUAL MASS FLUX IN HORIZONTAL TWO-PHASE FLOW.

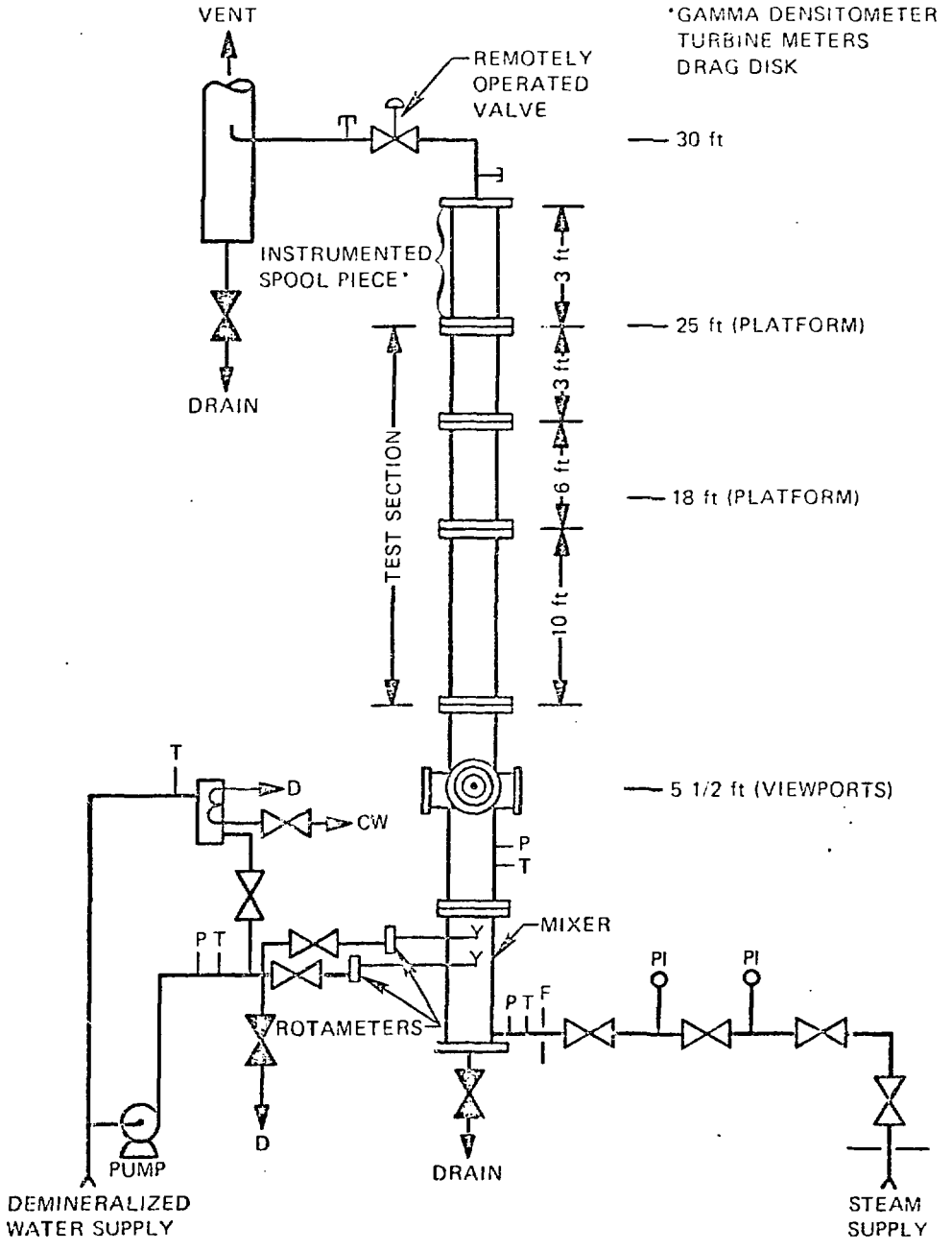

FIG. 19. AIRS STEAM WATER TEST STAND.

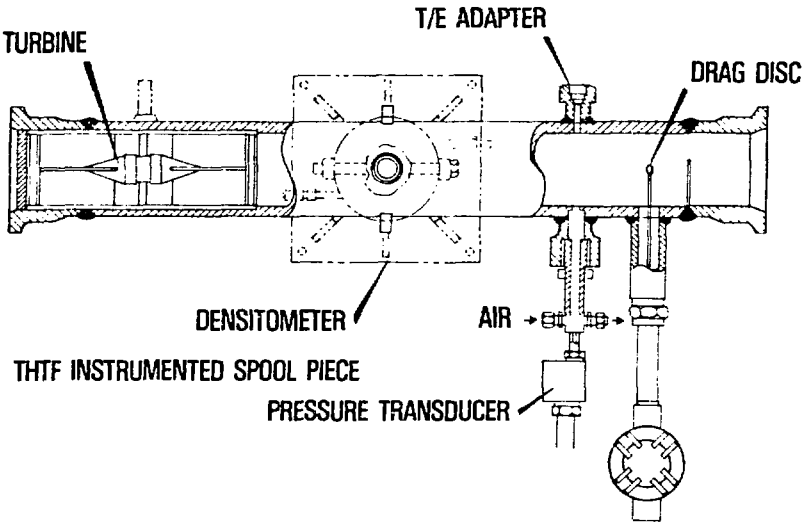

FIG. 20. INSTRUMENTED SPOOL PIECE USED IN STEADY STATE STEAM WATER TESTS.

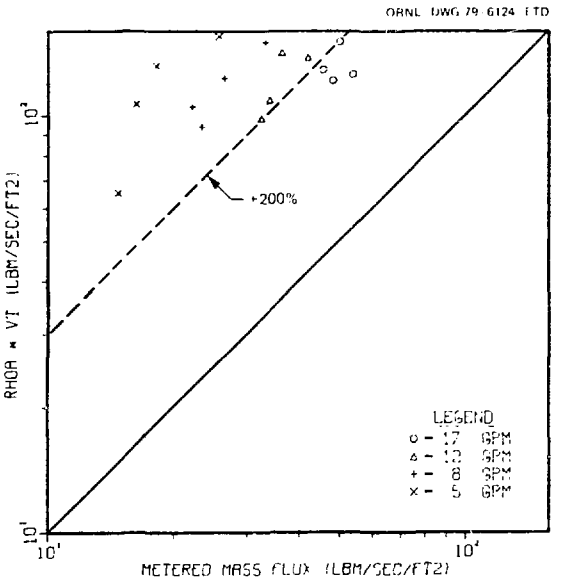

FIG. 21. MASS FLUX DETERMINED USING DENSITOMETER AND TURBINE METER VS METERED MASS FLUX, STEAM-WATER VERTICAL UPFLOW.

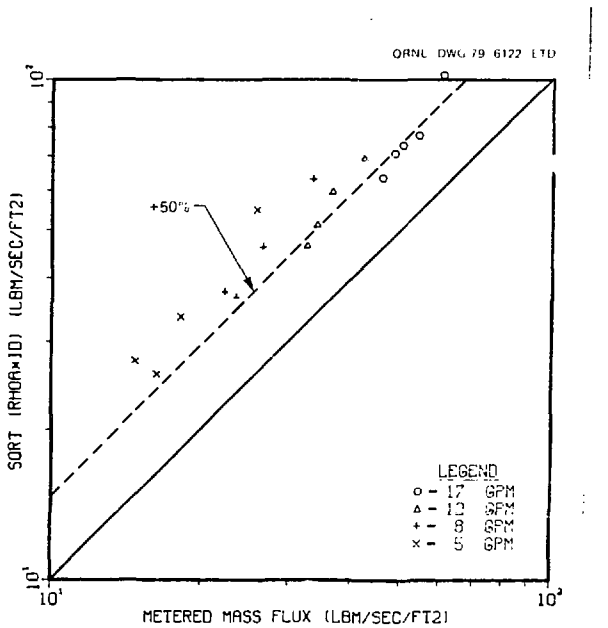

FIG. 22. MASS FLUX DETERMINED USING DENSITOMETER AND DRAG FLOWMETER VS METERED MASS FLUX, STEAM-WATER VERTICAL UPFLOW.

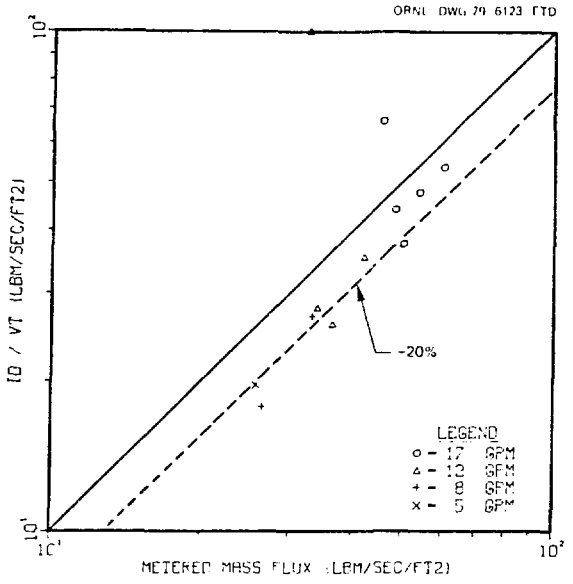

FIG. 23. MASS FLUX DETERMINED USING TURBINE AND DRAG FLOWMETER VS METERED MASS FLUX, STEAM-WATER VERTICAL UPFLOW.

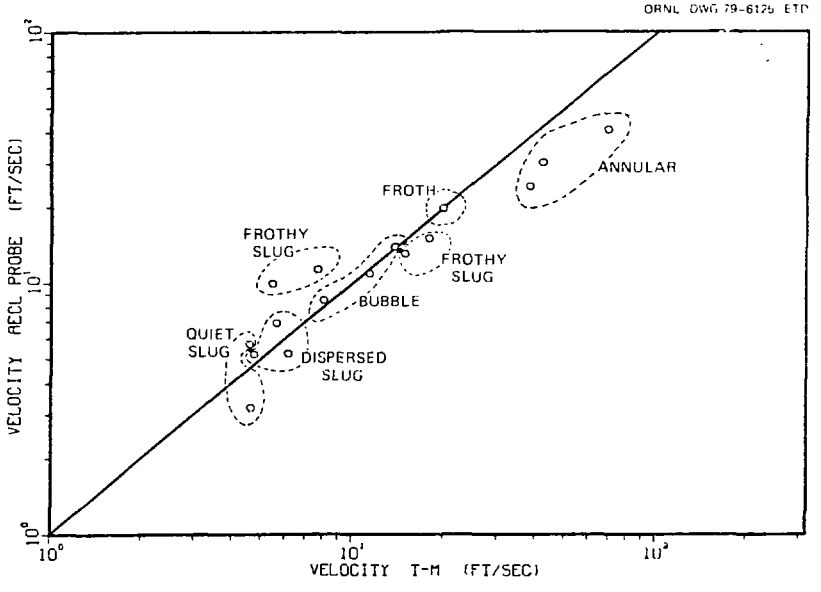

FIG. 25. VELOCITIES OBTAINED BY CROSS-CORRELATION WITH ACCL PROBES VS VELOCITIES INDICATED BY TURBINE, TWO-PHASE VERTICAL UPFLOW.

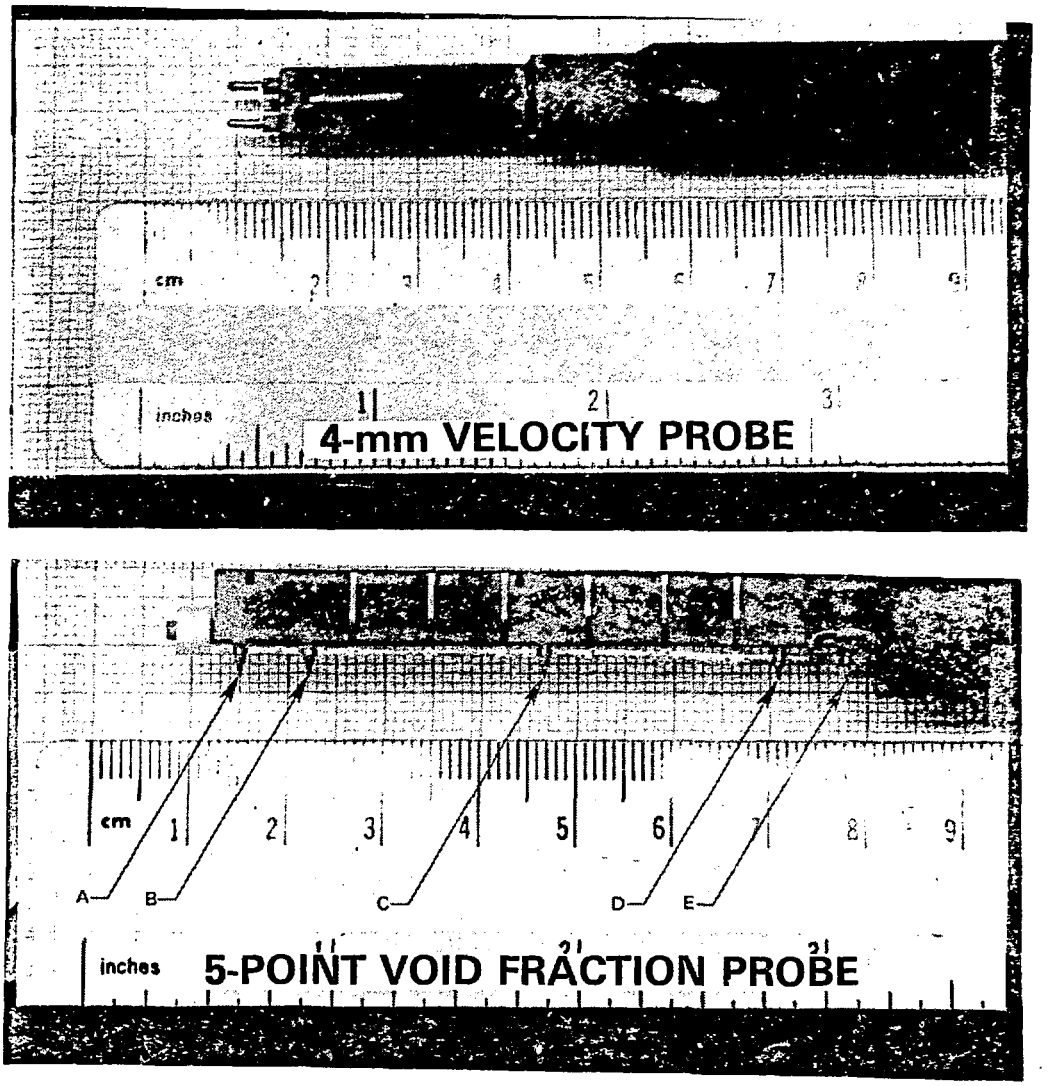

fig. 24. LOCAL CONDUCTIVITY PROBES.

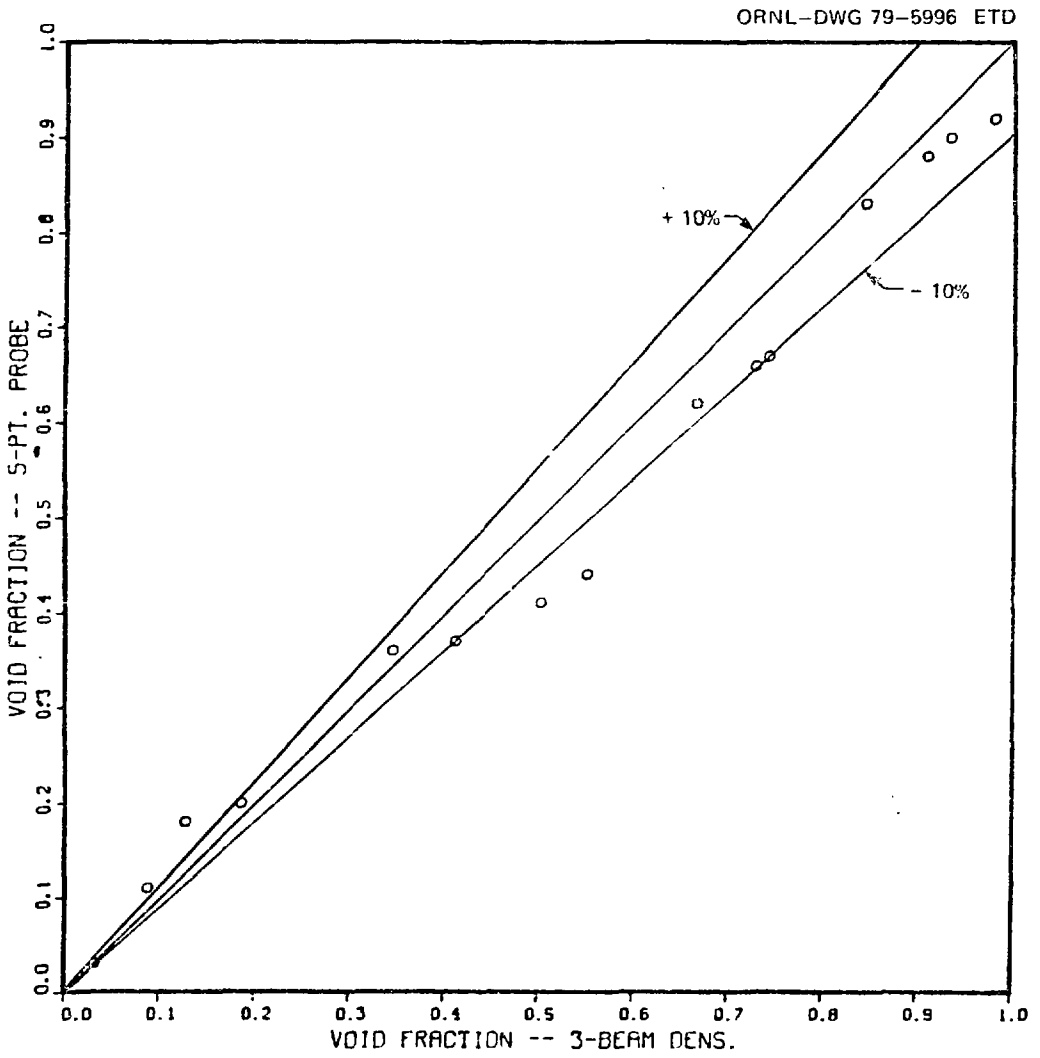

FIG. 26. MEAN PIPE VOID FRACTIONS OBTAINED WITH FIVE-POINT CONDUCTIVITY PROBE VS VOID FRACTION FROM DENSITOMETER, TWO-PHASE VERTICAL UPFLOW.

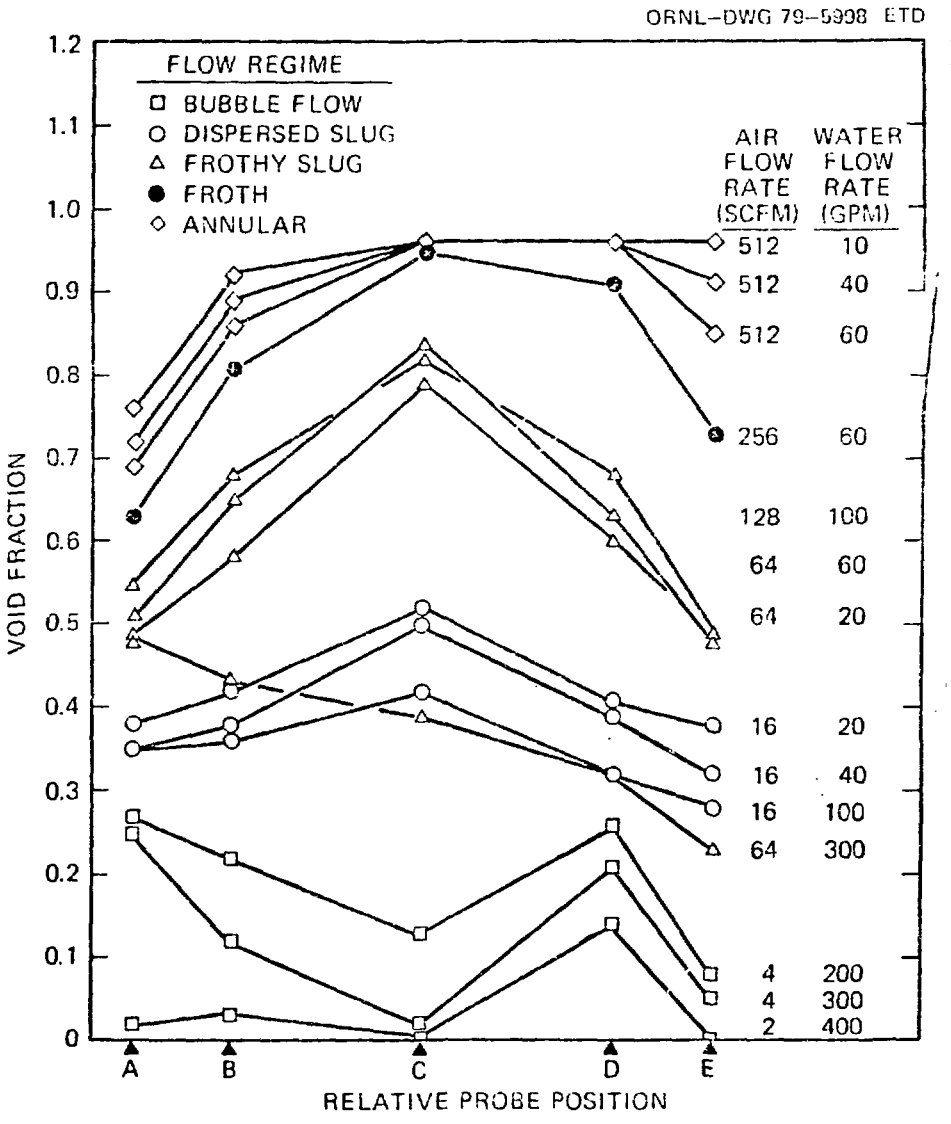

FIG. 27. LOCAL VOID FRACTION OBTAINED WITH FIVE-POINT CONDUCTIVITY PROBE IN AIR-WATER VERTICAL UPFLOW TESTS.